Supporting information

Significance of perylene for source allocation of terrigenous organic matter in aquatic sediments

Ulrich M. Hanke[1,*], Ana L. Lima-Braun[1,‡], Timothy I. Eglinton[1,2], Jeffrey P. Donnelly[3], Valier Galy[1], Pascale Poussart[1,†], Konrad Hughen[1], Ann P. McNichol[3], Li Xu[3], Christopher M. Reddy[1]

[1] Department of Marine Chemistry and Geochemistry, Woods Hole Oceanographic Institution, 266 Woods Hole Road, Woods Hole, MA 02543, USA

[2] Geological Institute, ETH Zürich, Sonneggstrasse 5, 8092 Zurich, Switzerland

[3] Department of Geology and Geophysics, Woods Hole Oceanographic Institution, Woods Hole Road, Woods Hole, MA 02543, USA

‡ Current address: ExxonMobil Exploration Company, Spring, Texas, USA

† Current address: Princeton University, 36 University Place, Princeton, New Jersey 08544 USA

*corresponding author: Ulrich M. Hanke, uhanke@whoi.edu

The supporting information includes details on the two-dimensional preparative capillary gas chromatographic isolation of PAHs for compound-specific isotope analysis, the concept of two modes of terrigenous organic matter export from land to oceans, the impact of the nuclear weapon testing on atmospheric and marine ^{14}C partitioning over time as well as results for grain size analyses.

Pages: 8
Figure: 3
Table: 2

Two-Dimensional Preparative Capillary Gas Chromatography (2D-PCGC)

Automated preparative capillary gas chromatography (PCGC) is a technique that allows the isolation and purification of specific compounds through repetitive injections (~100) of a mixture on a modified capillary gas chromatograph. Because the Pettaquamscutt River extracts were extremely rich in biogenic organic compounds, a sizable number of interfering compounds were still present in the PAH fractions, even after the intensive silica column and high-pressure liquid chromatography (HPLC) cleanup. This hindered the isolation of pure individual compounds by one-dimensional PCGC.

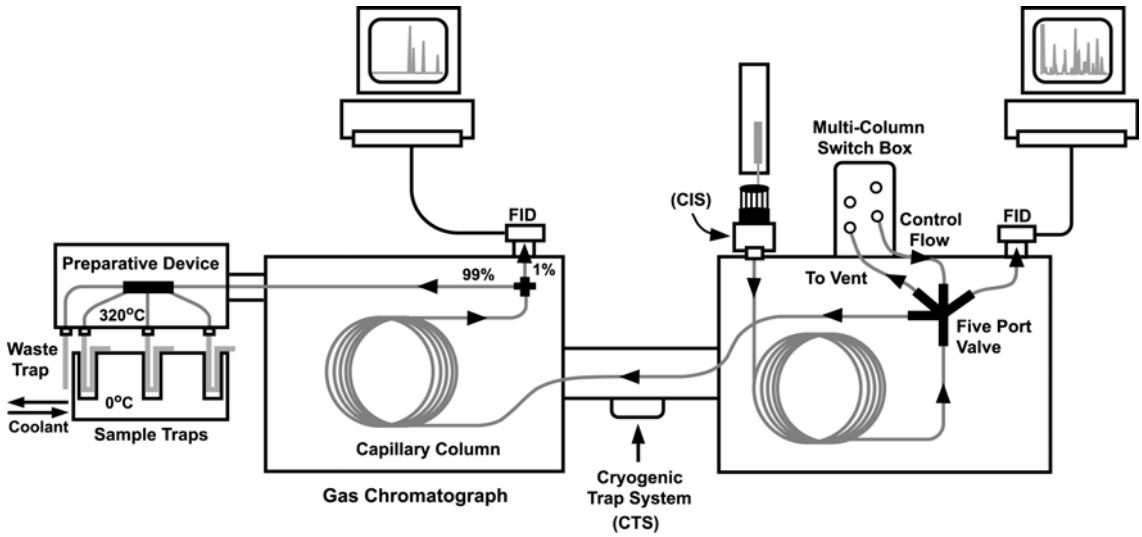

Figure 1. Schematic of a two-dimensional preparative capillary gas chromatograph (2D- PCGC).

In order to separate the PAHs from other organic compounds and isolate individual PAH isomers, we utilized a 2D-PCGC system (Figure 1). This instrument works in the same manner as the 1D-PCGC, with the advantage that incompletely separated components can be diverted from the first GC and fully resolved on the second GC equipped with a different stationary phase (Table 1), eliminating undesirable compounds in the process. In this study we used a HP 7683 auto-injector and a multi-column switching system (Gerstel MCS 2) that are connected to the first HP 6890 series gas chromatograph, and a Gerstel preparative fraction collector (PFC) is located at the end of the second GC. Similar to a 1D-PCGC, 1% of the effluent from the GC column is directed to a flame ionization detector (FID), so that compound separation and variations on retention times can be evaluated. The retention time windows correspond to components of interest and are transferred from the first GC to a cryogenic trap system, where the compounds are retained before injection

into the second GC. After separation on the second column, individual compounds are directed to the PFC for collection in cryogenically-cooled U-tube traps. Of the seven traps present in the PFC, six are used to collect compounds of interest and the 7th trap (waste trap) receives the remainder of the mixture. After isolation, the trapped PAHs were transferred from the U-tubes to 2-mL glass vials by addition of 1 mL of dichloromethane. Approximately 50-100 µL of each extract was transferred to a GC vial for determination of purity, concentration and stable carbon isotopic composition, while the remaining portion was purified for subsequent radiocarbon determination.

Table 1. Chromatographic conditions used in the first and second GC of the 2D-PCGC system for separation of individual PAHs.

Ring Class	Column GC1 and Temperature Program	Column GC2 and Temperature Program
3, 4-Ring PAHs	DB-35ms 60 m x 0.53 mm x 0.50 µm 60ºC (15 min hold) to 180ºC at 20ºC min^{-1}, and then from 180ºC to 320ºC at 5ºC min^{-1} (15 min hold)	DB-1 60 m x 0.53 mm x 1 µm 80ºC (40 min hold) to 180ºC at 20ºC min^{-1}, and then from 180ºC to 320ºC at 4.5ºC min^{-1} (4 min hold)
5, 6, 7-Ring PAHs	DB-1 60 m x 0.53 mm x 1 µm 80ºC (1.5 min hold) to 240ºC at 20ºC min^{-1}, and then from 240ºC to 325ºC at 5ºC min^{-1} (9 min hold)	DB-35ms 60 m x 0.53 mm x 0.50 µm 120ºC (38 min hold) to 240ºC at 20ºC min^{-1}, and then from 240ºC to 325ºC at 4ºC min^{-1} (15 min hold)

Concept of two modes of terrigenous organic matter export from land to ocean.

Natural biogeochemical cycles link the terrestrial with the aquatic environment including the surface and subsurface run-off of water following gravitational forces. Organic matter is produced in the biosphere either in soils or enters the soil column as litter. Some molecules survive the sequential degradation of organic matter from macro-scale tissues to biopolymers, monomers and ultimately CO_2, and rather are exported off-site than mineralized. Because of their refractory nature, they are referred to as molecular markers and facilitate tracing the spatial and temporal processes in the environment. Here we focus on the transport trajectory of carbon molecules in catchment soils prior to its export and subsequent burial in aquatic sediments.

Conventional ^{14}C source apportionment relies on isotope mass balance calculations with two-endmembers (contemporary biomass and fossil fuel-derived or petrogenic carbon), which has proven a powerful tool in aerosol science (short duration of transport) and large-scale geochemical assessments (other uncertainties outweigh the local dynamics). On local scale, however, it is necessary to consider export scenarios as well: 1. the event run-off during heavy precipitation and possible atmospheric transport (decadal); and 2. the continuous sub-surface flow, erosion of soil mineral horizon and re-/mobilization of organic matter from the soil column (millennial).

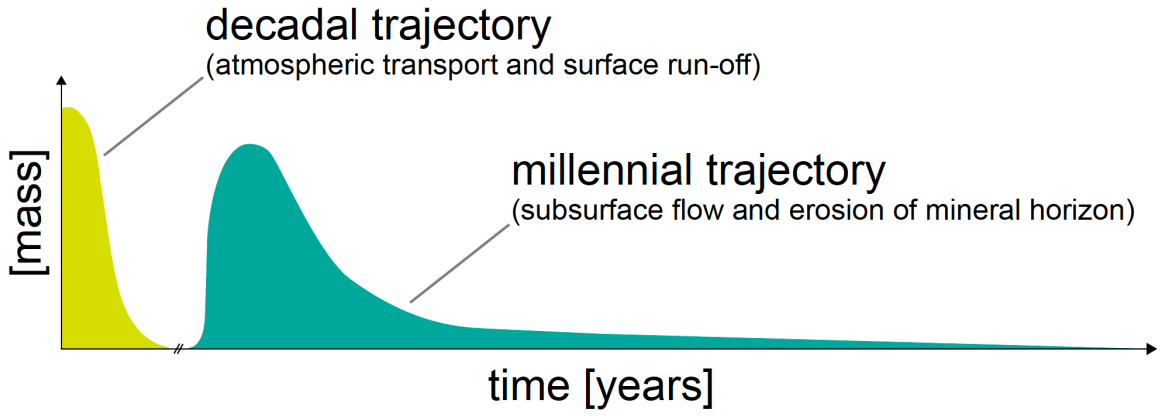

Figure 2. Conceptual illustration of different modes of organic matter export from catchment soils that is used to determine the contribution of terrigenous organic matter in aquatic sediments.

We factored those two processes in a simple mixing model of which we published the details in a previous study [1]. In brief, terrigenous organic matter is supplied on different time scales: a decadal (10 ± 10 %) and a millennial (90 ± 10 %) trajectory. The dominance of the millennial pool is empirically derived from a negative exponential function describing a mixture of ^{14}C values. This yields a “mean residence time” and implies that about 50 % of a molecular species is younger than the pre-aged value while the remaining 50 % are not older than ~10’000 years in this area due to the absence of post-glacial erosion. Our model explains more than 98 % of ^{14}C values that were ~16 % lower than the corresponding atmospheric ^{14}C content. The above-mentioned uncertainty of 10 % was chosen to account for natural variabilities caused by land-use change, natural disasters or simply shifts in climate.

Impact of the nuclear weapon testing on atmospheric and marine ^{14}C partitioning during the Anthropocene

Radiocarbon is a naturally occurring instable isotope ($T_{1/2}$ = 5730 years) of carbon that is produced in the upper atmosphere and is evenly distributed in the atmosphere on a sub-decadal scale. Depending on environmental factors such as steady cosmic matter fluxes or biosphere activity, the production rate equals the decay rate. However, while the terrestrial biosphere incorporates the atmospheric isotopic almost instantly, the coastal and surface oceans reveal ~5 % lower radiocarbon contents due to continuous phase-interchange of ^{14}C depleted dissolved inorganic carbon in the global marine environment.

With the onset of the industrialization, however, the Anthropocene began, and human activity altered the natural systems through the large-scale combustion of fossil fuels as well as the thermo-nuclear weapon testing in the mid-20th century. Both significantly disturbed the natural carbon signatures in our environment whereby the first diluted the natural ^{14}C contents ('Suess-Effect') and the second added ^{14}C to the atmosphere that nearly a doubled natural ^{14}C signatures for a short period of time (Figure 3).

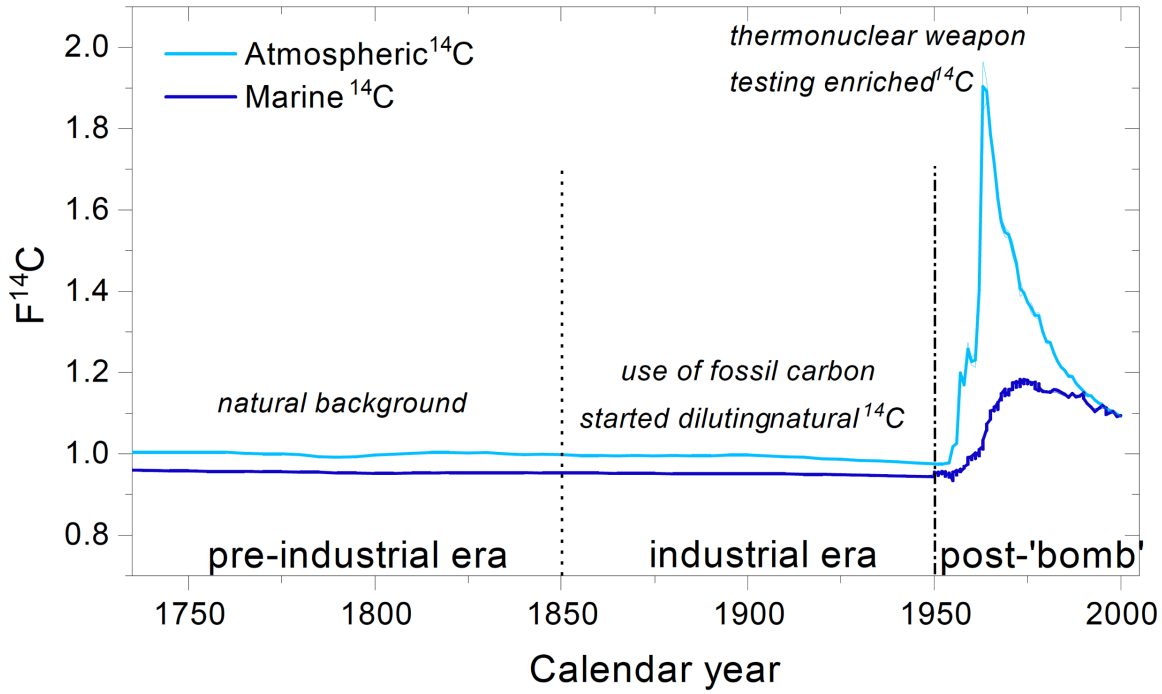

Figure 3. Northern hemisphere ^{14}C reference profiles throughout the Anthropocene with reference to the extended atmospheric Intcal13 and Marine13 data [2–5]; 14C contents are shown as fraction modern carbon.

The sharp increase in the atmospheric ^{14}C contents between ~1953 and ~1963 and the immediate decline thereafter evidences the instantaneous response of the atmospheric reservoir. In contrast, the response of the marine curve is delayed and much less pronounced than in the atmosphere. Thus, the marine ^{14}C responds slower thereby muting the drastic atmospheric changes. Further, the impact of the "Suess Effect" is less apparent in comparison to the consequences of the "bomb spike" (Figure 3). However, this dilution process is ongoing and has contributed significantly to the decline in ^{14}C concentrations since the international ban on surface thermonuclear weapon tests.

The burial of organic matter in coastal sediments records the legacy of aquatic and terrestrial productivity. The human disturbance of the natural ^{14}C contents, manifests itself in geochronological records and provide a stratigraphic marker for sedimentary sequences [6]. However, while ^{14}C measurements of organic carbon on bulk-level reveal the ‘bomb-spike’, this information is not reflected in our results on source-specific terrigenous markers, perylene and *n*-alkanoic acids. This apparent mismatch between molecular and bulk-level data is due to the different time-scales that control the supply of organic matter from land to ocean. While aquatic algae become buried on annual time-scale, the mobilization, transport and effective export of soil organic matter into depocenter of catchments is a complex process that links the terrestrial and aquatic environment on decadal to millennial time-scale.

We use the term ‘pre-aging’ to describe the lag time between production and burial yielding the catchment mean residence time. This value characterizes a catchment and can vary in different locations, for example because of geomorphology.

Individual data for grain size analyses

Table 2. Results for grain size analyses with Beckman Coulter LS13 320 Laser Diffraction Particle Analyzer after mineralization of organic matter with hydrogen peroxide.

Calendar year	Mid-point depth [cm]	Particle size distributions [µm]			
		D10 (lower 10 %)	D50 (median)	D90 (upper 10 %)	Surface Area [m^2 g^{-1}]
1996	1.5	1.89 ± 0.03	7.56 ± 0.18	23.51 ± 0.56	1.36 ± 0.02
1991	4.5	1.96 ± 0.08	7.97 ± 0.52	24.21 ± 1.04	1.31 ± 0.05
1986	7.8	2.16 ± 0.13	9.02 ± 0.71	26.87 ± 1.14	1.19 ± 0.07
1979	11.1	2.02 ± 0.02	8.31 ± 0.12	26.38 ± 1.34	1.26 ± 0.01
1973	14.3	2.16 ± 0.04	8.63 ± 0.12	24.64 ± 0.59	1.21 ± 0.02
1965	17.5	1.96 ± 0.10	7.88 ± 0.40	24.24 ± 0.67	1.28 ± 0.06
1956	20.7	1.98 ± 0.07	8.24 ± 0.23	27.52 ± 0.73	1.28 ± 0.04
1948	24.0	1.97 ± 0.09	8.37 ± 0.61	26.34 ± 1.69	1.29 ± 0.06
1938	27.3	1.99 ± 0.05	7.83 ± 0.40	23.45 ± 0.89	1.31 ± 0.04
1927	30.2	2.21 ± 0.20	10.37 ± 1.31	32.71 ± 1.24	1.14 ± 0.10
1916	32.4	2.01 ± 0.07	8.63 ± 0.25	28.58 ± 1.18	1.26 ± 0.04
1905	34.7	2.05 ± 0.09	8.18 ± 0.80	24.31 ± 2.28	1.27 ± 0.07
1894	37.0	2.17 ± 0.09	8.90 ± 0.79	25.82 ± 2.28	1.20 ± 0.06
1885	39.0	1.89 ± 0.10	7.11 ± 0.57	21.77 ± 1.14	1.39 ± 0.08
1878	41.0	1.91 ± 0.07	7.20 ± 0.35	22.15 ± 0.26	1.37 ± 0.05
1869	43.2	2.02 ± 0.07	7.69 ± 0.53	22.43 ± 1.19	1.30 ± 0.05
1860	45.4	1.89 ± 0.07	7.10 ± 0.35	21.55 ± 0.59	1.39 ± 0.05
1847	47.8	1.86 ± 0.05	7.28 ± 0.56	23.07 ± 2.65	1.39 ± 0.06
1830	51.5	1.93 ± 0.02	7.52 ± 0.21	23.31 ± 1.02	1.35 ± 0.02
1807	56.5	1.97 ± 0.11	8.15 ± 0.71	25.49 ± 1.80	1.30 ± 0.07

References

(1) Hanke, U. M.; Reddy, C. M.; Braun, A. L. L.; Coppola, A. I.; Haghipour, N.; McIntyre, C. P.; Wacker, L.; Xu, L.; McNichol, A. P.; Abiven, S.; Schmidt, M. W. I.; Eglinton, T. I. What on Earth Have We Been Burning? Deciphering Sedimentary Records of Pyrogenic Carbon. *Environ. Sci. Technol.* **2017**, *51* (21), 12972–12980. https://doi.org/10.1021/acs.est.7b03243.

(2) Levin, I.; Kromer, B.; Hammer, S. Atmospheric D14CO2 Trend in Western European Background Air from 2000 to 2012. *Tellus B* **2013**, *65* (20092), 1–7. https://doi.org/10.3402/tellusb.v65i0.20092.

(3) Levin, I.; Kromer, B. The Tropospheric 14CO2 Level in Mid Latitudes of the Northern Hemisphere. *Radiocarbon* **2004**, *46* (3), 1261–1272. https://doi.org/10.1017/s0033822200033130.

(4) Reimer, P. J.; Bard, E.; Bayliss, A.; Beck, J. W.; Blackswell, P. G.; Ramsey, C. B.; Buck, C. E.; Cheng, H.; Edwards, R. L.; Friedrich, M.; Grootes, P. M.; Guilderson, T. P.; Haflidason, H.; Hajdas, I.; Hatté, C.; Heaton, T. J.; Hoffmann, D. L.; Hogg, A. G.; Hughen, K. A.; Kaiser, K. F.; Kromer, B.; Manning, S. W.; Niu, M.; Reimer, R. W.; Richards, D. A.; Scott, E. M.; Southon, J. R.; Staff, R. A.; Turney, C. S. M.; van der Pflicht, J. Intcal13 and Marine13 Radiocarbon Age Calibration Curves 0-50,000 Years Cal BP. *Radiocarbon* **2013**, *55* (4), 1869–1887. https://doi.org/10.2458/azu_js_rc.55.16947.

(5) Andrews, A. H.; Asami, R.; Iryu, Y.; Kobayashi, D. R.; Camacho, F. Bomb-Produced Radiocarbon in the Western Tropical Pacific Ocean: Guam Coral Reveals Operation-Specific Signals from the Pacific Proving Grounds. *J. Geophys. Res. Ocean.* **2016**, *121*, 6351–6366. https://doi.org/10.1002/2016jc012043.

(6) Lima, A. L.; Hubeny, J. B.; Reddy, C. M.; King, J. W.; Hughen, K. A.; Eglinton, T. I. High-Resolution Historical Records from Pettaquamscutt River Basin Sediments: 1. 210Pb and Varve Chronologies Validate Record of 137Cs Released by the Chernobyl Accident. *Geochim. Cosmochim. Acta* **2005**, *69* (7), 1803–1812. https://doi.org/10.1016/j.gca.2004.10.009.